

# The Proapoptotic Influenza A Virus Protein PB1-F2 Forms a Nonselective Ion Channel

Michael Henkel<sup>1</sup>, David Mitzner<sup>2</sup>, Peter Henklein<sup>3</sup>, Franz-Josef Meyer-Almes<sup>4</sup>, Anna Moroni<sup>5</sup>, Mattia L. DiFrancesco<sup>5</sup>, Leonhard M. Henkes<sup>1</sup>, Michael Kreim<sup>1</sup>, Stefan M. Kast<sup>6</sup>, Ulrich Schubert<sup>2,7</sup>, Gerhard Thiel<sup>1\*</sup>

**1** Department of Botany, Technische Universität Darmstadt, Darmstadt, Germany, **2** ViroLogik GmbH, Innovation Centre for Medical Technology and Pharmaceuticals (IZMP), Erlangen, Germany, **3** Institute of Biochemistry, Humboldt University, Berlin, Germany, **4** Department of Chemistry and Biotechnology, Hochschule Darmstadt, Darmstadt, Germany, **5** Dipartimento di Biologia e IBF-CNR, Università degli Studi di Milano, Milano, Italy, **6** Physikalische Chemie III, Technische Universität Dortmund, Dortmund, Germany, **7** Clinical and Molecular Virology, Friedrich-Alexander-University of Erlangen-Nürnberg, Erlangen, Germany

## Abstract

**Background:** PB1-F2 is a proapoptotic influenza A virus protein of approximately 90 amino acids in length that is located in the nucleus, cytosol and in the mitochondria membrane of infected cells. Previous studies indicated that the molecule destabilizes planar lipid bilayers and has a strong inherent tendency for multimerization. This may be correlate with its capacity to induce mitochondrial membrane depolarization.

**Methodology/Principal Findings:** Here, we investigated whether PB1-F2 is able to form ion channels within planar lipid bilayers and microsomes. For that purpose, a set of biologically active synthetic versions of PB1-F2 (sPB1-F2) derived from the IAV isolates A/Puerto Rico/8/34(H1N1) (IAV<sub>PR8</sub>), from A/Brevig Mission/1/1918(H1N1) (IAV<sub>SF2</sub>) or the H5N1 consensus sequence (IAV<sub>BF2</sub>) were used. Electrical and fluorimetric measurements show that all three peptides generate in planar lipid bilayers or in liposomes, respectively, a barely selective conductance that is associated with stochastic channel type fluctuations between a closed state and at least two defined open states. Unitary channel fluctuations were also generated when a truncated protein comprising only the 37 c-terminal amino acids of sPB1-F2 was reconstituted in bilayers. Experiments were complemented by extensive molecular dynamics simulations of the truncated fragment in a lipid bilayer. The results indicate that the c-terminal region exhibits a slightly bent helical fold, which is stable and remains embedded in the bilayer for over 180 ns.

**Conclusion/Significance:** The data support the idea that PB1-F2 is able to form protein channel pores with no appreciable selectivity in membranes and that the c-terminus is important for this function. This information could be important for drug development.

**Citation:** Henkel M, Mitzner D, Henklein P, Meyer-Almes F-J, Moroni A, et al. (2010) The Proapoptotic Influenza A Virus Protein PB1-F2 Forms a Nonselective Ion Channel. PLoS ONE 5(6): e11112. doi:10.1371/journal.pone.0011112

**Editor:** Ralph Tripp, University of Georgia, United States of America

**Received:** March 10, 2010; **Accepted:** May 24, 2010; **Published:** June 15, 2010

**Copyright:** © 2010 Henkel et al. This is an open-access article distributed under the terms of the Creative Commons Attribution License, which permits unrestricted use, distribution, and reproduction in any medium, provided the original author and source are credited.

**Funding:** GT received funding from Deutsche Forschungsgemeinschaft, SMK from Adolf-Messer-Stiftung and the Fonds der Chemischen Industrie, and AM from European Drug Initiative on Channels and Transporters (EDICT). The funders had no role in study design, data collection and analysis, decision to publish, or preparation of the manuscript.

**Competing Interests:** The authors have declared that no competing interests exist.

\* E-mail: thiel@bio.tu-darmstadt.de

## Introduction

Influenza A Virus (IAV) is a permanent threat to humans and animals with the potential to cause disastrous pandemics which appeared periodically in the last century causing millions of fatal casualties [1,2]. Aquatic birds are the primary reservoir of the virus. Some avian strains are able to infect other mammals or humans directly or after genetic reassortment caused by a process termed antigenic shift [3]. A major role is attributed to pigs which serve as “mixing vessel” that create avian-human reassortant strains, of pandemic potential. The recent flu pandemic caused by a influenza A virus strain of swine origin is of high interest to study the dynamics of virulence and viral spread. Though, much effort was made to unravel the precise mechanisms of IAV mediated pathogenicity in different host organisms leaving many questions to understand this complex process. Only a few years ago an 11<sup>th</sup> IAV gene product was discovered. The new protein, named PB1-

F2 originates from an alternative open reading frame in the PB1 polymerase gene and it is present in most human and bird flu isolates [4,5].

Recent work has established that PB1-F2 is an important pathogenicity factor, since it has the potential to augment the generation of fatal secondary bacterial pneumonia as it was demonstrated after the expression of the 1918 IAV PB1-F2 protein in infected mice [6]. Furthermore, a single amino acid exchange from Asn-66 to Ser-66 converted an H5N1 strain of moderate pathogenicity into a highly pathogenic virus. This mutation was also found in the PB1-F2 protein of the 1918 pandemic virus isolate [7]. Interestingly, H1N1 isolates of swine origin do not express functional PB1-F2, which might be a reason for the so far reported moderate pathogenicity of the new subtype variant [8].

The complete mode of action of PB1-F2 however is not yet fully understood. The protein exhibits a C-terminal mitochondrial targeting sequence (MTS) and is predominantly localized in the



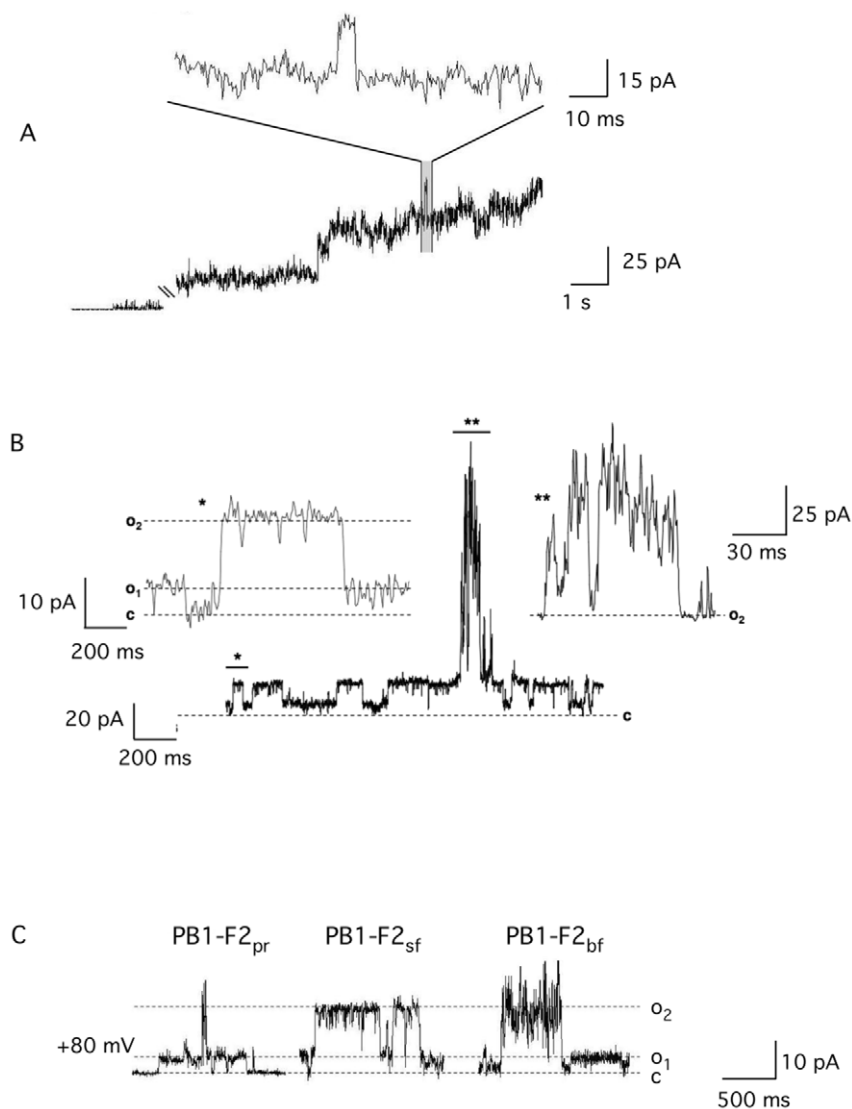


**Figure 2. sPB1-F2 evoked membrane conductance.** (A) Addition of sPB1-F2<sub>pr8</sub> protein at 1  $\mu$ M to the trans side of a planar lipid bilayer results in current fluctuations. In the present case only occasionally clear channel like fluctuations (see expanded trace) are resolvable on the background of many unresolved fluctuations. (B) In a majority of experiments the conductance fluctuates in a channel like manner between a closed (c) and two defined conductance levels  $o_1$  and  $o_2$ . Transitions between the two conductance levels (\*) are expanded in the left inset. The channel like fluctuations are occasionally interrupted by burst like events (\*\*), which reveal also at higher magnification (inset on the right) no resolvable conductance levels. doi:10.1371/journal.pone.0011112.g002

with some other more rare occurring conductance levels at all voltages. Fig. 3A illustrates exemplary traces of unitary channel activity from an experiment with symmetrical 500 mM KCl. The two conductance levels are frequently achieved directly from the closed state. However the fluctuations illustrated in Fig. 3B show that the channel can also reach the closed state from the high conductance level  $o_2$  via an intermediate halt at the small conductance level  $o_1$  (B); also partial closures in which the current decreases in step like fashion from  $o_2$  can be observed (C). From these data we can conclude that the different conductance levels are causally related; they must be produced by the same protein or protein complex.

A plot of the two prevailing unitary current amplitudes from the closed level to  $o_1$  and to  $o_2$  as a function of voltages gives a linear current/voltage (I/V) relation for both levels of conductance in symmetrical 500 mM KCl (Fig. 3D). The conductance of the large and the small unitary opening are 250 pS and 100 pS respectively.

The same results were confirmed in 4 other reconstitution experiments using protein from two different preparations.

To test whether the channel forming activity is unique to sPB1-F2<sub>pr8</sub> the same experiments were repeated with synthetic peptide analogs to PB1-F2 from the ‘Spanish flu’ virus (sPB1-F2<sub>sf</sub>) and the bird flu virus (H5N1) (sPB1-F2<sub>bf</sub>). An alignment of the three protein sequences shows that they are 60% identical (Fig. 1). Direct comparison however also reveals deviations in the amino acid sequence throughout the protein; furthermore PB1-F2<sub>bf</sub> is at the c-terminus 3 amino acids shorter than the two analogs.

Fig. 3E shows exemplary current traces at +80 mV from the three different peptides. The data reveal that all three peptides generate distinct channel fluctuations. In all cases the two dominant conductance levels  $o_1$  and  $o_2$  are again observable. The I/V curves obtained for sPB1-F2<sub>sf</sub> and sPB1-F2<sub>bf</sub> are indistinguishable from sPB1-F2<sub>pr</sub> (Fig. 3D).

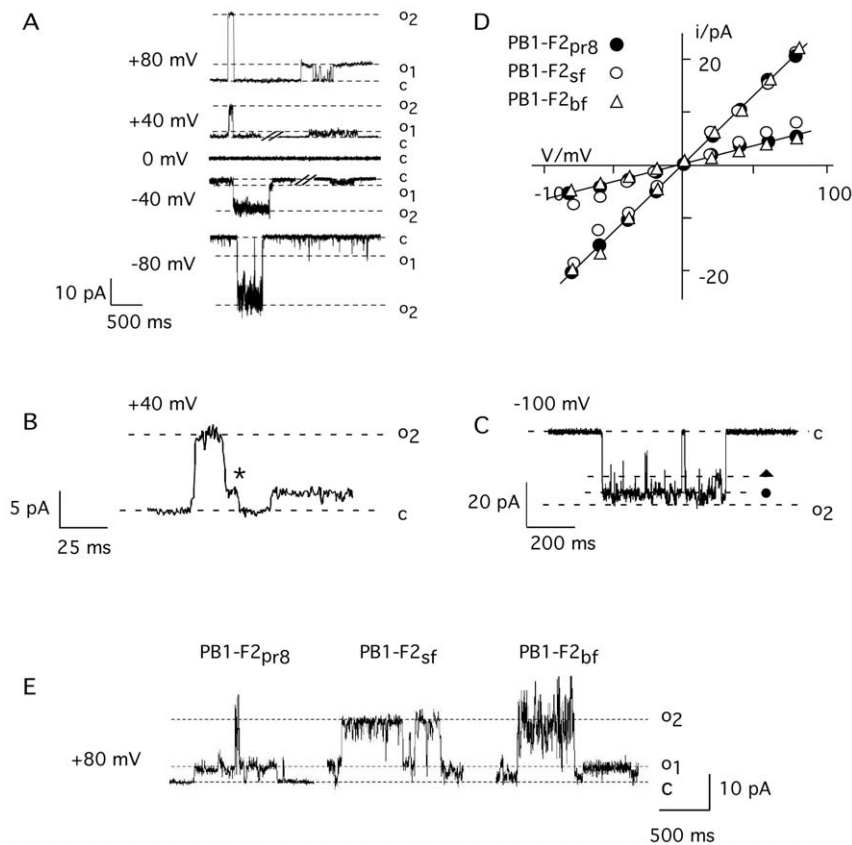


**Figure 3. Unitary channel fluctuations and current voltage relation of sPB1-F2<sub>pr8</sub> generated conductance in planar lipid bilayer.** Current fluctuates between a closed (c) and two ( $o_1$ ,  $o_2$ ) conductance levels (A). Channel fluctuations recorded in symmetric 500 mM KCl in trans and cis chamber. (B) Example of channel opening in one step between closed (c) and maximal conductance ( $o_2$ ) and closing with an intermediate rest at low conductance level (\*). (C) Example of intermediate closures from maximal conductance ( $o_2$ ) to sub-conductance levels, which are indicated by symbols (●, ▲). (D) I/V relation of the small ( $o_1$ ) and large current fluctuation ( $o_2$ ). Experiments performed in symmetrical 500 mM KCl. The I/V relations in D were obtained from measurements of channel conductance evoked by peptide from sPB1-F2<sub>pr8</sub>, sPB1-F2<sub>sf</sub> and sPB1-F2<sub>bf</sub>. (E) examples of channel type current fluctuations between the closed (c) and two conductance levels ( $o_1$ ,  $o_2$ ) evoked by sPB1-F2 peptide from influenza Puerto Rico strain (sPB1-F2<sub>pr8</sub>), Spanish flu strain (sPB1-F2<sub>sf</sub>) and bird flu strain (sPB1-F2<sub>bf</sub>). Measurements in A-C were done in symmetric 500 mM KCl in trans and cis chamber at a voltage of +80 mV; all peptides were added to the buffer at final concentration of 1  $\mu$ M.  
doi:10.1371/journal.pone.0011112.g003

To test the selectivity of the sPB1-F2<sub>pr8</sub> generated channel for different ions the experiments were repeated under non-symmetrical conditions. The I/V relations obtained in experiments in which KCl in the cis chamber was replaced by either NaCl or by K-gluconate were similar to those obtained with symmetrical KCl (Fig. 4A). This means that the channel has no apparent selectivity; it neither discriminates appreciably between  $K^+$  and  $Na^+$  nor between  $Cl^-$  and gluconate.

Further experiments were performed with a 10-fold concentration gradient of KCl across the bilayer. The current voltage relation obtained for sPB1-F2<sub>pr8</sub> under these non-symmetrical conditions reverses close to 0 mV at ca +5 mV. This shift in reversal voltage is real because under non-symmetrical conditions we were able to measure a negative current at 0 mV. The result of this experiment implies that the channel transports anions slightly better than cations.

In further experiments we tested whether the viral protein also transports divalent ions. For these experiments sPB1-F2<sub>sf</sub> or sPB1-F2<sub>pr8</sub> were reconstituted in a planar lipid bilayer with 500 mM KCl on the cis and 500 mM  $CaCl_2$  on the trans side. Also in these experiments we were able to detect distinct current fluctuations at positive and negative voltages (Fig. 4C and inset). The results of these experiments show that the sPB1-F2 generated conductance is also permeable to  $Ca^{2+}$ .

During long observations it occurred that current fluctuations were more frequent at more extreme voltages than at moderate voltages. This suggested a voltage dependency of the sPB1-F2 generated conductance. In order to quantify the channel activity as a function of voltage we estimated the mean current generated by sPB1-F2<sub>pr8</sub> in a bilayer from  $n = 25$  voltage steps of 3 s duration from 0 mV to test voltages between +80 mV and -80 mV. The mean steady-state currents from 12 experiments recorded in symmetrical 500 mM KCl are plotted in Fig. 5 as a function of voltage. They show a low activity at voltages around 0 mV. Towards both voltage extremes channel activity increases in a quasi-exponential fashion. Similar results were obtained with sPB1-F2<sub>sf</sub>; also this protein exhibits a voltage dependent I/V relation of the mean current (Fig. 5). The results of this analysis show that channel activity is irrespective of the viral origin of the sPB1-F2 protein favoured by membrane voltage. It is not possible to say whether the proteins insert into the bilayer with respect to its orientation randomly or with a bias for one side over the other. Without this information it is not yet possible to discriminate whether the channel has an inverse bell shaped open probability or whether they function as a rectifier.

The NMR structure obtained for sPB1-F2<sub>pr8</sub> implies a c-terminal  $\alpha$ -helix, which is long enough to span a membrane [13].

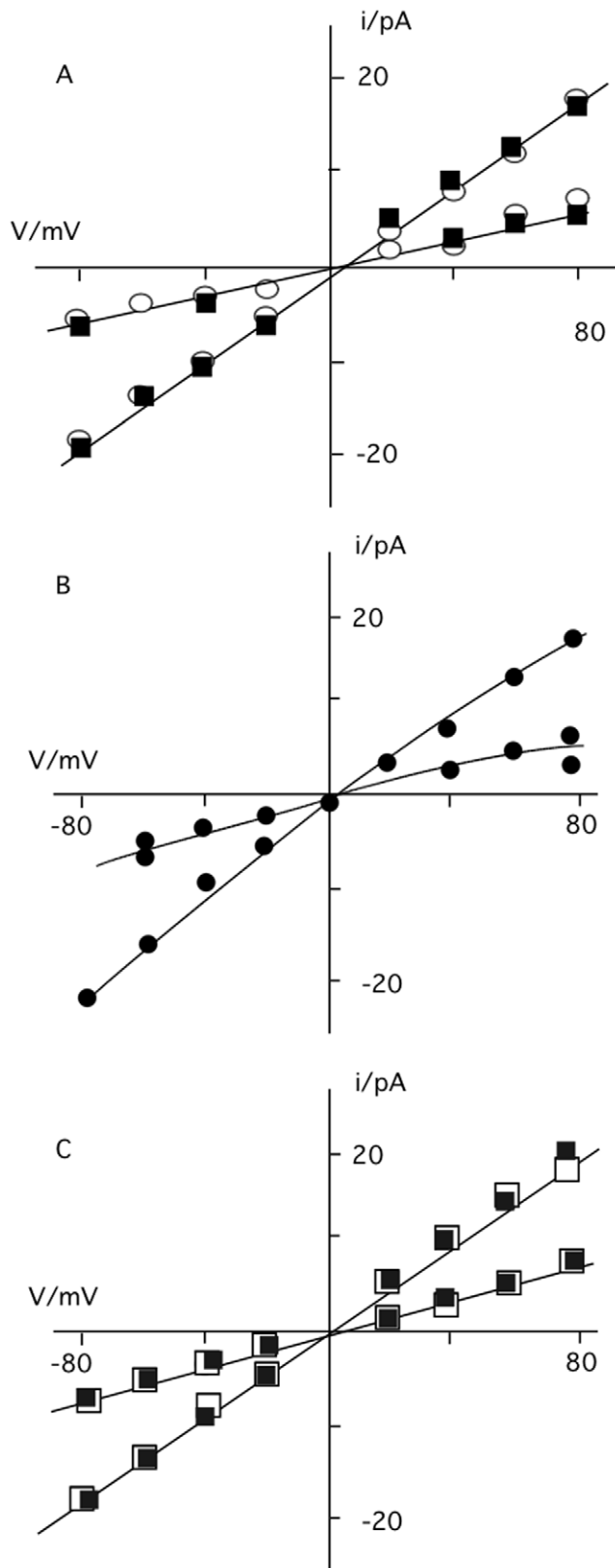


**Figure 4. I/V relation of the small ( $o_1$ ) and large ( $o_2$ ) sPB1-F2 generated current fluctuation.** (A) Unitary currents were recorded in bilayer with 500 mM KCl on *trans* side and 500 mM NaCl on *cis* (open circles) or with 500 mM KCl on *cis* and 500 mM K-gluconate on *trans* (filled squares). (B) I/V relation obtained with 500 mM KCl on *trans* side and 50 mM KCl on *cis* side. (C) I/V relation obtained with 500 mM

KCl on *cis* and 500 mM CaCl<sub>2</sub> on *trans* side. Currents were elicited upon adding sPB1-F2<sub>pr8</sub> (in A-C) and sPB1-F2<sub>sf</sub> (in C) to *trans* side. doi:10.1371/journal.pone.0011112.g004

In order to test whether this domain alone is sufficient for generating channel activity we produced a synthetic peptide, which is equivalent to the aa 50–87 of the full-length protein of PB1-F2<sub>pr8</sub> [15]. The peptide (sPB1-F2<sub>pr8</sub><sup>50–87</sup>) was tested in planar lipid bilayer in the same way as the full-length protein. Fig. 6 shows the result of a typical experiment with a symmetrical solution of 500 mM KCl; the membrane was clamped to +80 mV. Addition of the truncated peptide at a concentration of >200 nM to the *trans* chamber generated a large conductance in the bilayer. The current generated by sPB1-F2<sub>pr8</sub><sup>50–87</sup> peptide showed mostly unresolved current fluctuations. But like in the experiment of Fig. 2A it was also in these experiments possible to resolve channel like fluctuations between defined conductance levels (Fig. 6). A plot of the resolvable channel like fluctuations reveals three distinct conductance levels with 330, 550 and 750 pS. These conductance levels are not identical to those recorded with the full-length protein. Hence the putative  $\alpha$ -helical part of the sPB1-F2 protein is sufficient to increase membrane conductance; it can even generate channel like activity. The difference in the resolvable conductance levels obtained with the full length compared to the truncated protein implies that the remaining n-terminal part of the protein has an influence on channel formation and unitary conductance.

#### Fluorescence assay

The electrophysiological data imply that the sPB1-F2 protein generates an unspecific conductance including permeation by Ca<sup>2+</sup> and Cl<sup>-</sup>. This offers the possibility to examine the transport properties of PB1-F2 also in an independent assay by fluorescence spectroscopy. To measure PB1-F2 generated Ca<sup>2+</sup> fluxes we loaded liposomes with the Ca<sup>2+</sup> sensitive dye Fluo-3. The fluorescence intensity of the dye remained constant under control conditions. Also addition of the K<sup>+</sup> selective ionophore Valinomycin had no appreciable effect on the Fluo-3 fluorescence. In contrast, addition of 1  $\mu$ M sPB1-F2<sub>pr8</sub> resulted in a rise in Fluo-3

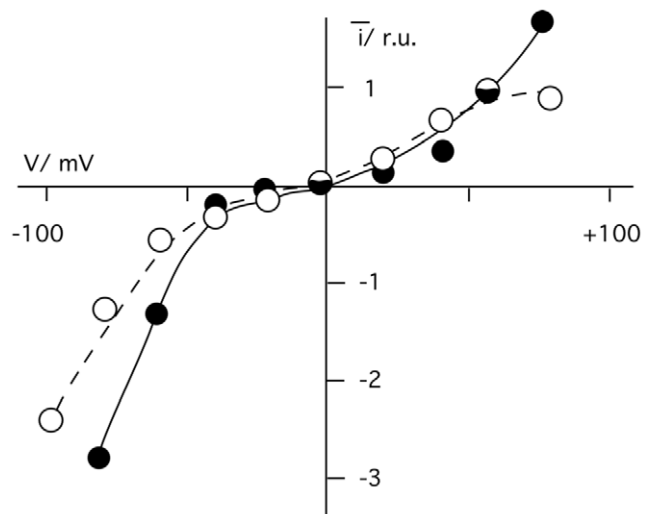


**Figure 5. Mean current generated by sPB1-F2<sub>pr8</sub> (filled circles) or sPB1-F2<sub>sf</sub> (open circles) as a function of voltage.** Channel activity was recorded in symmetrical 500 mM KCl. Peptide was added at 1  $\mu$ M on *trans* side. The current responses from  $n=12$ , 3 sec long voltage scans at the respective test voltages were averaged. doi:10.1371/journal.pone.0011112.g005

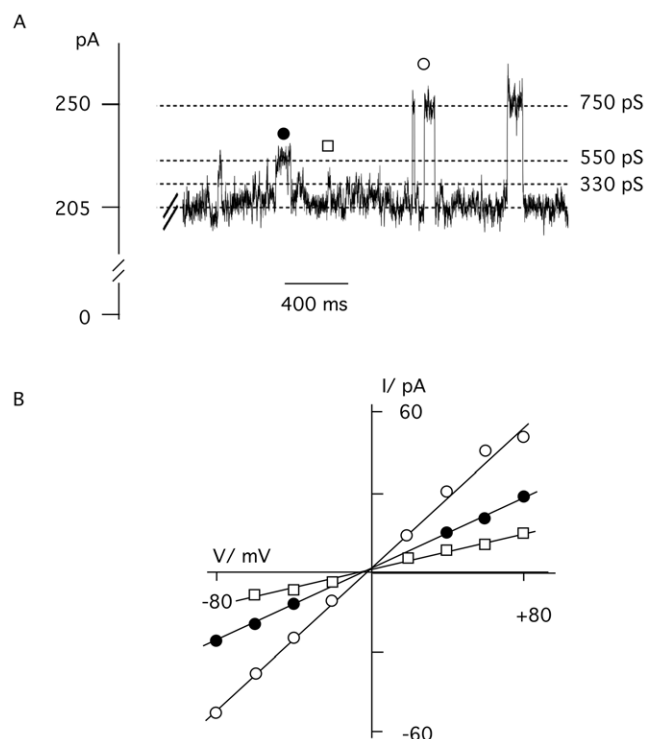


**Figure 6. The truncated peptide sPB1-F2<sub>pr8</sub><sup>50-87</sup> generates an elevated membrane conductance.** A: Addition of sPB1-F2<sub>pr8</sub><sup>50-87</sup> protein to the trans side of a planar lipid bilayer evokes large currents across the membrane. On top of many unresolved current fluctuations typical channel like opening and closing events are resolvable. In the example recorded at +80 mV three distinct current levels (indicated by different symbols) can be identified. B: a plot of similar resolvable current levels as a function of voltage reveals three linear I/V relations with 330, 550 and 750 pS. The symbols in A cross reference with symbols in B. Measurements were done in symmetric 500 mM KCl with 200 nM peptide concentration.  
doi:10.1371/journal.pone.0011112.g006

fluorescence indicating a net influx of Ca<sup>2+</sup> into the liposomes (Fig. 7). The sPB1-F2<sub>pr8</sub> generated fluorescence signal could be increased by adding the peptide together with Valinomycin (Fig. 7). This enhancing effect of the ionophore on Ca<sup>2+</sup> influx into the liposomes is expected because a K<sup>+</sup> efflux via Valinomycin provides a charge balance for Ca<sup>2+</sup> influx. In this case the membrane of the liposomes is not building up a charge, which would hinder net Ca<sup>2+</sup> influx.

With a similar assay we also tested whether the truncated peptide sPB1-F2<sub>pr8</sub><sup>50-87</sup> is able to generate a Ca<sup>2+</sup> conductance. For this purpose we loaded liposomes with Fluo-3 and measured the respective fluorescence before and after adding sPB1-F2<sub>pr8</sub><sup>50-87</sup> peptide to the incubation buffer. The exemplary data in Fig. 7B show that the fluorescence signal was constant before addition of the peptide. The addition of sPB1-F2<sub>pr8</sub><sup>50-87</sup> at a final concentration of 1 μM resulted in a quasi-immediate rise in Fluo-3 fluorescence reporting the influx of Ca<sup>2+</sup> into the liposomes. The increase of relative fluorescence units (RFU) was 30%. The same response with a mean rise of 28 ± 5% in Fluo-3 fluorescence was observed in 3 other experiments.

In further experiments we also examined the ability of sPB1-F2<sub>pr8</sub> to stimulate Cl<sup>-</sup> fluxes. In this case the liposomes were loaded with the anion sensitive dye lucigenin. Other than with Fluo-3 we observed in this type of experiments a non-specific drift of the fluorescence signal. But in spite of this shortcoming also this

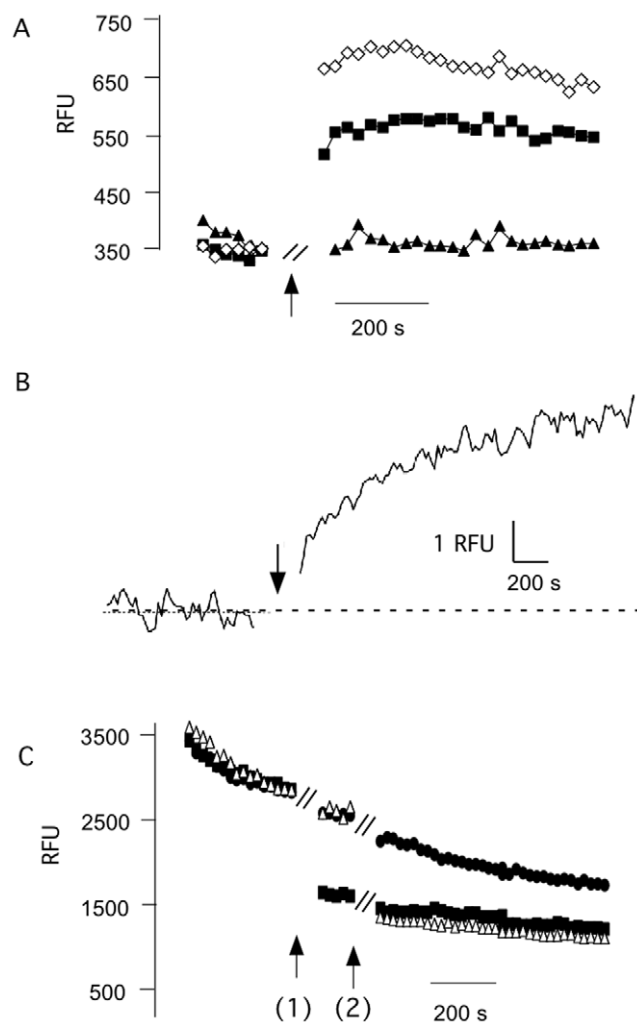


**Figure 7. sPB1-F2 generates Ca<sup>2+</sup> and anion fluxes into liposomes.** (A) Fluorescence of liposomes with Ca<sup>2+</sup> sensitive dye Fluo3 was recorded before and after adding (at arrow) ionophore Valinomycin (triangle), sPB1-F2<sub>pr8</sub> alone (filled squares) or together with Valinomycin (open squares). Peptide and ionophore were added during the time gap of ca. 1 min indicated in the graph. The presence of the peptide results in an increase in fluorescence indicating an influx of Ca<sup>2+</sup> into the liposomes. The ionophore enhances Ca<sup>2+</sup> influx because it prevents building up of a charge, which hinders net Ca<sup>2+</sup> influx. (B) Fluorescence of liposomes filled with Ca<sup>2+</sup> sensitive dye Fluo-3 before and after addition (at arrow) of 1 μM peptide to incubation medium. The truncated peptide sPB1-F2<sub>pr8</sub><sup>50-87</sup> results in a fast rise in Fluo3 fluorescence. (C) Fluorescence of liposomes filled with anion sensitive dye lucigenin was measured before and after adding of anion specific ionophore TBT (filled squares, added at arrow 1), sPB1-F2<sub>pr8</sub> (open triangle, arrow 2). The control was left untreated (filled circles); the stepwise drop of the control signal is due to an unspecific drift of the signal. Both ionophore and sPB1-F2<sub>pr8</sub> generate a strong quenching of the lucigenin fluorescence well beyond the control indicating an influx of anions. Peptide and ionophore were added during the time gap of ca. 1 min indicated in the graph.  
doi:10.1371/journal.pone.0011112.g007

method could be used to demonstrate PB1-F2 generated anion fluxes. Fig. 7C shows that addition of the anion specific ionophore TBT resulted in a strong quenching of the lucigenin fluorescence indicating the sensitivity of the system. A similar drop in fluorescence was obtained upon addition of sPB1-F2<sub>pr8</sub> at a concentration of 1 μM.

Collectively, the results of these experiments confirm the electrophysiological data in that the sPB1-F2 protein is able to generate a conductance without appreciable selectivity in lipid bilayers, which is able to conduct anions and divalent cations. The c-terminal domain of the protein with its putative  $\alpha$ -helical structure seems to be sufficient for generating this conductance.

### MD simulation

The electrical data imply that PB1-F2 is able to form with its c-terminus ion channels in membranes. A prerequisite for such channel formation is an insertion and a lasting transmembrane orientation of the c-terminus. To test the latter we examined the behavior of the peptide in its proposed  $\alpha$ -helical form in a lipid environment at zero transmembrane voltage by molecular dynamics (MD) simulations. After a period with fixed center of mass of the c-terminal truncated fragment sPB1-F2<sub>pr6</sub><sup>50-87</sup> we observed the stability of the truncated protein by a number of quantitative measures over the last 180 ns after removal of the center-of-mass (c.o.m.) constraint. This constraint has been applied during pre-equilibration in order to fix the protein within the membrane. Quantitative results are shown in Fig. 8. All quantities indicate a remarkable overall stability of the protein fold and of the transmembrane insertion geometry. Apparently, the protein structure fluctuates within expected margins, but there is no indication for a systematic long-term trend to escape from the bilayer or to switch to a different backbone fold.

While particularly the helical characteristic is preserved, we note a tendency to bend slightly in comparison with the NMR structure, most notable at around 70 ns where a slight step in the observables is visible. This process started shortly after removal of the c.o.m. constraint and is visualized in Fig. 9 (note that the simulation box shrinks laterally even after long time, indicating that large time scales are required for reaching an equilibrium ensemble). Bending is not unexpected since Pro<sup>67</sup> is localized near the centre of the peptide. Interestingly, the Pro<sup>67</sup> appears to be conserved within 263 bird flu sequences and all 20 of the H1N1 full length sequences analysed by us so far (data not shown). However, the presence of a lipid environment apparently hinders the formation of a kink. The origin of this behavior is related to the presence of a large number of positively charged amino acids (all kept in the standard protonation state during the simulation) as illustrated in Fig. 10. Arginine and lysine residues tend to “snorkel” into the direction of the membrane/solvent interface [16]. Close to the c-terminus (bottom side in Figs. 9 and 10) positive charges are clustered which leads to a net tendency to drag the protein in the direction of the c-terminus. In the presence of the c.o.m. constraint, this force is neutralized, whereas, in the absence of the constraint, the smaller number of positive charges on the n-terminal side is not sufficient to counteract fully. As a consequence, stabilization of the n-terminal side in the interface decreases such that the influence of proline becomes more important which leads to the observed bending.

It appears that the c-terminal cluster of positive charges leads to an accumulation of water and anions, which penetrate the lipid head groups. There is no indication of a persistent poration effect, however, which could be responsible for the measured channel currents. This observation requires further investigation in future work considering oligomers of the PB1-F2 peptide.

### Discussion

Early studies described PB1-F2 as a proapoptotic protein, which was assumed to remove host immune cells responding to IAV infection [4,11]. The molecular mechanisms of PB1-F2 induced

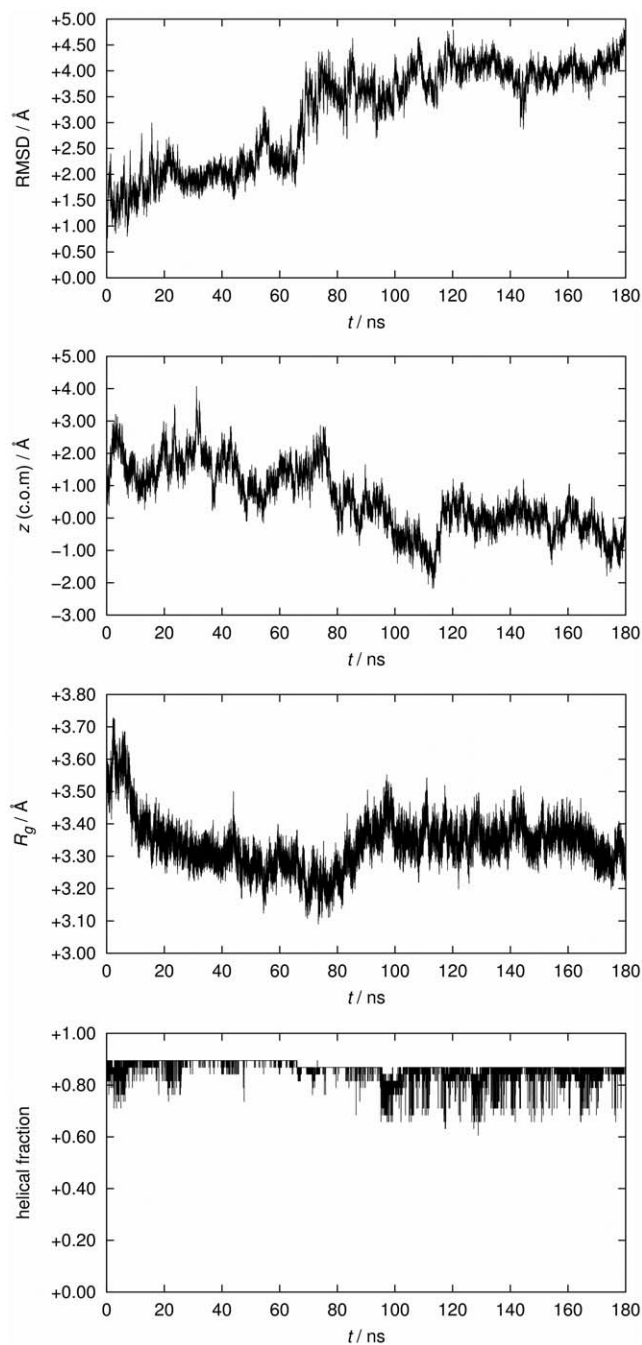


**Figure 8. Dependence of various measures for protein stability over the simulation time after removal of the center-of-mass (c.o.m.) constraint (set to 0 ns).** From top to bottom: Root mean square deviation (RMSD) of the protein backbone, z coordinate (membrane normal) of the c.o.m. of the protein (corrected by removing the total membrane drift), the protein's radius of gyration ( $R_g$ ), and the helical fraction recognized for the fold. doi:10.1371/journal.pone.0011112.g008

apoptosis is still not totally understood, though recent results confirmed that its proapoptotic function is cell specific and related to PKC activation after infection of primary human monocytes [17]. However, since the protein is localized predominantly in the mitochondria of transfected or infected cells and found to alter the mitochondrial morphology [4] it was hypothesized that apoptosis induction occurs due to direct interaction with subunits of the



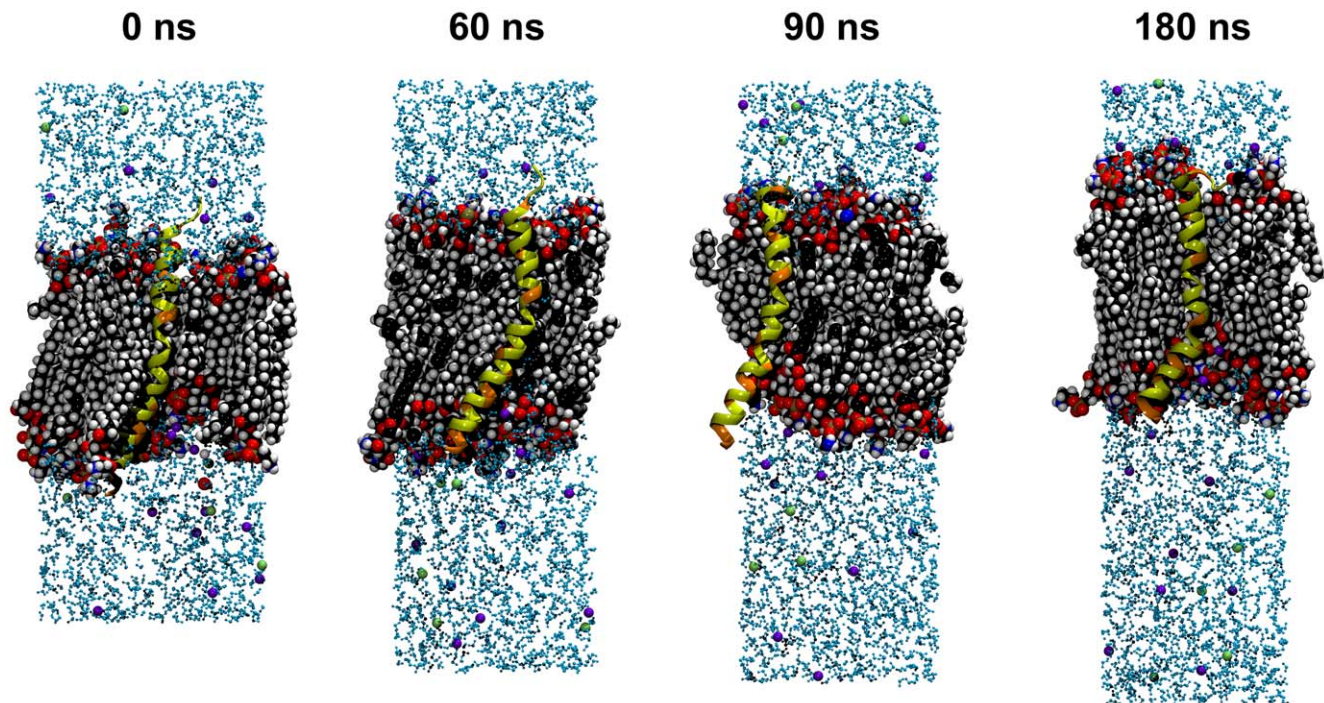


**Figure 9. Snapshots of the simulation system after removal of the center-of-mass constraint (set to 0 ns).** The protein is shown in cartoon representation with the location of positively charged amino acids marked by orange color. Potassium ions are shown in green, chloride ions in blue. The c-terminus is located on the bottom side.  
doi:10.1371/journal.pone.0011112.g009

mitochondrial PTPC or destabilisation of the mitochondrial membrane by pore formation [10].

In previous experiments it has been demonstrated that PB1-F2 causes an elevation of membrane leakage [14] and increases the electrical conductance of membranes [12]. However, the currents elicited by the PB1-F2 protein were not showing defined conductance levels and channel like fluctuations. The results of these experiments therefore fostered the hypothesis that the PB1-F2 protein is not forming canonical protein mediated transmembrane pores. It was speculated that the protein may destabilize the lipid bilayer due to the formation of lipidic pores [12]. The question of how this protein destabilizes the mitochondrial membrane potential, by channel like or lipidic pore formation, is still under investigation.

The main observation of the present study is that the PB1-F2 protein is able to generate distinct opening/closing events between defined conductance levels; these events are typical for ion channel proteins [18]. Thus, it can be concluded that PB1-F2 can short circuit the mitochondria by inserting channel forming proteins into the organelle membrane. This finding might explain the property of PB1-F2 to disrupt the reticulotubular mitochondrial organization and to dissipate the inner membrane potential [4,10]. A similar strategy for inducing apoptosis is known from a number of other viruses [19]. In the case of PB1-F2 canonical channel activity is observed with the full-length protein but also with a truncated protein comprising only the putative c-terminal  $\alpha$ -helix (from amino acid residues Ile<sup>55</sup>-Lys<sup>85</sup>). This together with the results from MD simulations, which show that the truncated fragment is stable in the membrane, suggests that the c-terminus is part of the channel forming domain in the protein. But since the truncated and the full-length protein evoke different unitary conductances we must nonetheless assume that also the n-terminal part of the protein is involved in channel formation. Indeed the simulations show that the

monomer alone leads to membrane denting, but is apparently incapable of inducing ion permeation; we did not find evidence for sufficient destabilization of the membrane to allow for passive ion translocation. Although we made no attempt to model a multi-protein complex, it is very likely that such a complex is necessary to facilitate ion transport. This hypothesis is supported by the finding that PB1-F2 has indeed the tendency to form oligomers. The latter involves distinct domains not only in the C- but also in the N terminus [13] in line with the hypothesis, that both termini are important for the complete channel activity.

Our MD simulations imply that the c-terminus of PB1-F2 can maintain a transmembrane orientation and that this orientation is favoured by positive amino acids at the membrane/water interfaces. The data however do not yet explain how a peptide with that many charges is able to insert into the membrane. In this context it is interesting to note that also many other short, highly cationic and hydrophilic peptides, including the voltage sensor of K<sup>+</sup> channels, are capable of inserting and in some cases even passing membranes [20–22]. The unusual behavior of these proteins can be explained by an interaction of the membrane with the distinct peptide structure; the charged amino acids in these membrane-inserting cationic peptides have to be evaluated in the overall context and their specific position in the entire peptide [20]. The structural and charge density features of the PB1-F2 protein are apparently similar to those of cationic peptides, which are able to insert spontaneously into membranes. Due to the large net charge it is very likely that the voltage dependency of the PB1-F2 conductance is related to a voltage-induced change of the positioning and orientation within the membrane. This issue needs further scrutiny by MD simulations employing an external transmembrane potential.

Both experimental and theoretical data support the view that channel activity is achieved by protein pores, which are formed by



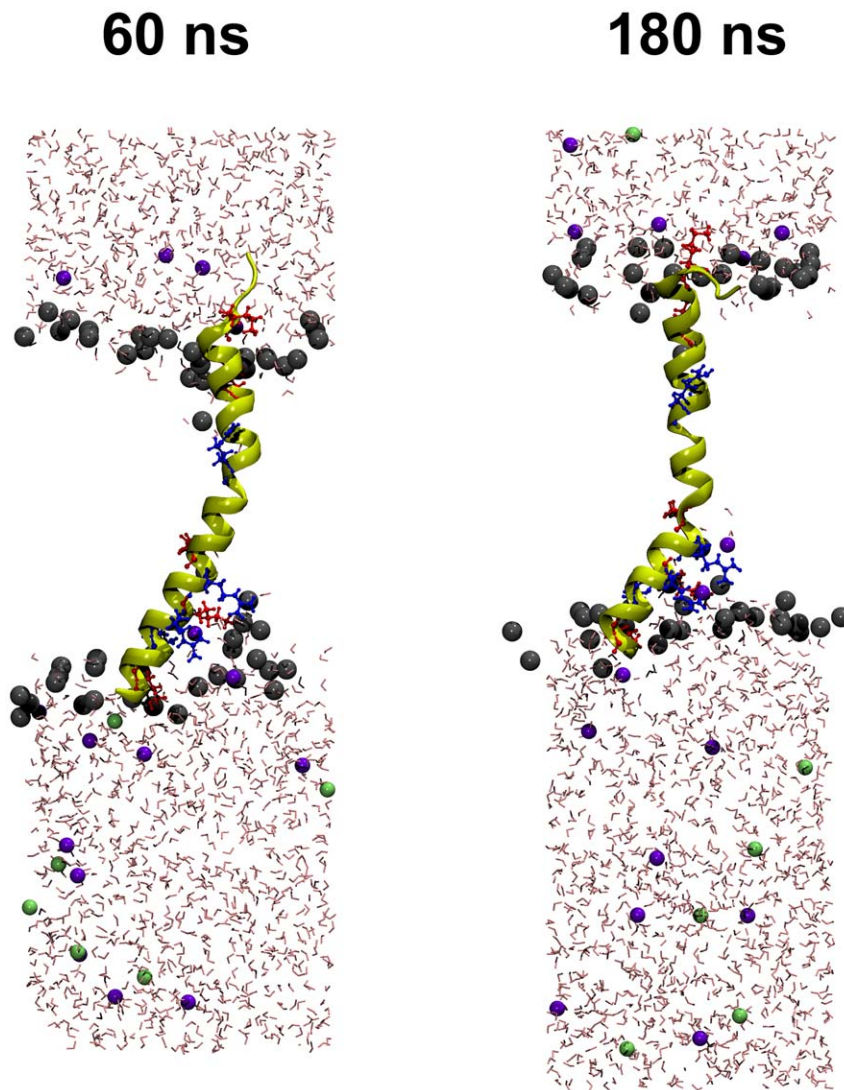


**Figure 10. Snapshots of the simulation system after removal of the center-of-mass constraint (set to 0 ns).** The protein is shown in cartoon representation with explicit depiction of positively charged residues (arginine: blue, lysine: red). Lipid molecules have been removed except for the head groups that are depicted as grey spheres. Potassium ions are shown in green, chloride ions in blue. The c-terminus is located on the bottom side. doi:10.1371/journal.pone.0011112.g010

complex formation of the PB1-F2 protein. The importance of the c-terminus for channel activity is consistent with the finding that similar channel fluctuations are observed here with all three PB1-F2 analogs. The three proteins are variable in length with an overall identity of ca. 60%. Important in the context of structure/function correlates is that all three analogs contain a similar c-terminal domain with a putative transmembrane  $\alpha$ -helix. Interestingly, all human H1N1 isolates circulating since 1950 were reported to code for a truncated PB1-F2 of 57 amino acids [5] lacking the c-terminal domain. Moreover, the current H1N1 swine flu isolates are not able to express any form of PB1-F2 since multiple Stop-codon mutations only allow the expression of the first 11 amino acids. This is consistent with initial findings that expression of PB1-F2 is species dependent and often interrupted in swine isolates [4]. Because of the missing c-terminal  $\alpha$ -helix these proteins are therefore most likely unable to generate channel function.

The fact that the PB1-F2 peptides derived from different isolates were all able to generate similar channel like activity in planar lipid

bilayers implies that the different PB1-F2 variants have the same potential of ion channel conductance within the mitochondria of infected cells. We can only speculate about the reasons why this channel type activity was recorded here but not in a previous study [12]. It is possible that the fusion efficiency of the peptides was in the present study lower than in a previous study. A lower number of proteins in the bilayer however can be beneficial for the resolution of single channel activity because individual events are not masked by the simultaneous activity of many channels. Also in the case of other pore forming peptides step like channel fluctuations can only be observed when the number of proteins inserted into the bilayer is low [20,23].

The analysis of PB1-F2 evoked unitary channel currents in buffers with different ion compositions reveals that the channel has two main conductance levels and both are non-selective; they transport cations as well as anions with a marginal preference for anions. The low selectivity of the channel and in particular the permeability to gluconate implies a very simple and wide channel pore. The tendency of PB1-F2 to form oligomers [13] presumably

results in a self-assembly of multiple monomers in membranes with a central water filled pore. Similar channel pores with low selectivity can also be formed by aggregation of small membrane proteins from other viruses [24–26] or by the aforementioned alamethicin [22].

One particular feature of the PB1-F2 induced channel activity is the occurrence of at least two defined conductance levels, which can be achieved directly from the closed state. This is not unique to PB1-F2 but can also be observed with other small channel forming membrane proteins such phospholamban [27]. Also the antibiotic peptide alamethicin generates multiple unitary current levels whose conductances obey a geometrical progression; each transition is thought to result from the uptake or release of an individual monomer within the conducting bundle [28]. This explanation however does not hold true for the PB1-F2 generated conductances because inspections of the current traces also revealed intermediate closures from the high conductance level to lower levels (see Fig. 2C). Such behaviour cannot be explained by dynamic uptake or release of individual monomers from a conducting bundle. We must hence conclude that the low conductance level is a real sub-state of a channel protein build with a fixed number of monomers.

Recent data stress that PB1-F2 has the potential to modulate IAV virulence. A single amino acid exchange in the c-terminal region of the protein from Asn66 to Ser66 is sufficient to convert a virus of moderate pathogenicity into a highly pathogenic one [7]. It was also found that the expression of the 1918 IAV PB1-F2 in mice enhanced secondary bacterial pneumonia [6]. This finding is important because most IAV related deaths are due to bacterial super-infection [6]. The present data show that the three PB1-F2 peptides from IAV of different pathogenic potential have in spite of their sequence differences the same ability to generate ion channel activity. Hence the difference in biological function between the three PB1-F2 proteins must be due to other properties such as mitochondrial targeting or association with other proteins. Notably, the two PB1-F2 proteins, which were derived from the PR8 isolate and from the Spanish flu isolate, differ in amino acid 66, which is a Ser in IAV<sub>SF2</sub> and an Arg in IAV<sub>PR8</sub> (Fig. 1); this mutation, which accounts for the difference in pathogenicity [7], is within the mitochondrial targeting sequence [9].

## Methods

### Reconstitution and Electrophysiology

Experiments with planar lipid bilayers were performed as described by Schrempf et al. [29] by the Montal-Müller technique [30] with a 0.4 mg/ml solution of  $\alpha$ -phosphatidylcholine (type IV-S> = 30% TLC; Sigma-Aldrich (Steinheim, Germany)) in n-decan (Carl Roth, Karlsruhe, Germany). sPB1-F2 was synthesized as described elsewhere [15,31]. The measurements were done in buffer containing 500 mM KCl, 10 mM Mops/Tris pH 7. The Ag/AgCl electrode of in the trans compartment was directly connected to the head stage of a current amplifier (EPC 7, List, Darmstadt, Germany). In order to prevent surface-potential-effects both electrodes were connected with the bath solution via an agar bridge (2% agarose in 2 M KCl). Currents were recorded and stored by an analog/digital-converter (LIH 1600, HEKA electronics, Germany) at 4 KHz after low pass filtering at 1 kHz. Data analysis were performed by Patchmaster-Software (HEKA electronics) and Igor Pro (WaveMetrics, Oregon, USA). Before adding the protein to the trans chamber the bilayer conductance was recorded for some time in order to exclude artefacts from contaminations. Only perfectly silent bilayers were used for reconstitution of PB1-F2 proteins.

### Preparation of liposomes for the fluorescence assay

Lipid mixtures (100 mg/ml, S IV lipid, Sigma) were dried from CHCl<sub>3</sub>-methanol (1/1) solution under vacuum. Dried lipids were re-suspended in buffer (100 mM KCl, 10 mM Mops, titrated with Tris to pH 7.0) by vortexing; after addition of 20  $\mu$ M fluorescence dye (Fluo-3, Invitrogen) liposomes were exposed to three freeze-thaw cycles. During thawing periods the liposomes were kept in an ultrasonic bath for 5 minutes. This procedure resulted in the loading of liposomes with dye. Finally the dye was removed from the external buffer by precipitation; 1ml of the dispersion was therefore washed on sephadex<sup>®</sup>-columns (Sigma Aldrich, Steinheim, Germany). The liposomes were subsequently eluted from the column by Na<sup>+</sup> buffer (100 mM NaCl, 10 mM Mops/Tris pH 7.0). Immediately before an experiment, the eluate was further diluted 1/4 with the Na<sup>+</sup> buffer. The fluorescence signals (Fig. 7A,B) were measured with a fluorescence microplate reader (NanoScan LF400, IOM, Berlin, Germany) or a fluorescence spectrophotometer (F-7000, HITACHI, Japan) (Fig. 7C). In the microplate experiments Fluo3 was excited at 488 nm and lucigenin at 456 nm. In both cases the emitted light passed through a 505 nm dichroic and a 520/10 band path filter. Fluo3 fluorescence measured in the fluorescence spectrophotometer was excited at 506 $\pm$ 5 nm and at an emission wavelength of 526 $\pm$ 5 nm.

### MD simulation

The system was constructed using VMD [32] and described by with the CHARMM22 potential function for proteins [33], CHARMM27 for phospholipids [34], the TIP3P water model [35], and ion parameters developed by Roux [36]. All titratable residues were kept at their standard protonation states. The simulation has been performed with a modified version of the program NAMD 2.6 [37]. Starting with the experimental NMR structure [13], the protein was inserted into a pre-equilibrated POPC membrane by removing overlapping lipid molecules, leading to 26 and 28 POPC molecules in each layer. The system was solvated by ca. 150 mM aqueous KCl solution (15 K<sup>+</sup> and 6 Cl<sup>-</sup> ions per 4050 water molecules), the positive net charge of the protein was therefore balanced by counterions. The total system contained 19641 atoms. The simulation time step was 2 fs, electrostatics were treated by the particle mesh Ewald method [38] on a 64x64x128 grid. Nonbonded real-space interactions were smoothly switched off over a range of 10–12 Å. Bond distances to hydrogen atoms were kept fixed. Production simulations were performed in the isothermal-isobaric ( $NpT$ ) ensemble using the Langevin piston algorithm at 1 atm [39,40] with an oscillation period of 800 fs and damping constant of 400 fs, and the Langevin thermostat with a coupling constant of 5 ps<sup>-1</sup>. After minimization over 10000 steps we successively turned on the barostat and the thermostat over 0.182 ns, followed by 5 ns  $NpT$  simulation with fixed protein backbone and 10 ns  $NpT$  simulation with c.o.m. constraint applied to the protein. Data for the fully free system were collected over 180 ns. The helicity of the protein backbone was analyzed with the STRIDE algorithm [41].

### Acknowledgments

Computer time was provided on the IBM Regatta system (Hessischer Hochleistungsrechner) at the Hochschulrechenzentrum Darmstadt.

### Author Contributions

Conceived and designed the experiments: DM AM US GT. Performed the experiments: MH FJMA MLD LMH MK. Analyzed the data: MH MLD LMH MK SMK. Contributed reagents/materials/analysis tools: DM PH. Wrote the paper: AM SMK US GT.

## References

- Lamb RA, Takeda M (2001) Death by influenza virus protein. *Nat Med* 7: 1286–1288.
- Yewdell J, Garcia-Sastre A (2002) Influenza virus still surprises *Curr Opin Microbiol* 5: 414–418.
- Webby RJ, Webster RG (2001) Emergence of influenza A viruses. *Philos Trans R Soc London B Biol Sci* 356: 1817–1828.
- Chen W, Calvo PA, Malide D, Gibbs J, Schubert U, et al. (2001) A novel influenza A virus mitochondrial protein that induces cell death. *Nat Med* 7: 1306–1312.
- Zell R, Krumbholz A, Eitner A, Krieg R, Halbhuber K-J, et al. (2007) Prevalence of PB1-F2 of influenza A viruses. *J Gen Virol* 88: 536–546.
- McAuley JL, Hornung F, Boyd KL, Smith AM, McKeon R, et al. (2007) Expression of the 1918 influenza A virus PB1-F2 enhances the pathogenesis of viral and secondary bacterial pneumonia. *Cell Host & Microbe* 2: 240–249.
- Conenello GM, Zamarin D, Perrone LA, Tumpey T, Palese P (2007) A single mutation in the PB1-F2 of H5N1 (HK/97) and 1918 influenza A viruses contribute to increased virulence. *Plos Pathogens* 3: 1414–1421.
- Schnitzler SU, Schnitzler P (2009) An update on swine-origin influenza virus A/H1N1. *Virus Genes* 39: 279–292.
- Gibbs JS, Malide D, Hornung F, Bennink JR, Yewdell JW (2003) The Influenza A Virus PB1-F2 Protein Targets the Inner Mitochondrial Membrane via a Predicted Basic Amphipathic Helix That Disrupts Mitochondrial Function. *J Virol* 77: 7214–7224.
- Zamarin D, Garcia-Sastre A, Xiao X, Wang R, Palese P (2005) Influenza Virus PB1-F2 protein induces cell death through mitochondrial ANT3 and VDAC1. *PLOS Pathogens* 1: 40–54.
- Lowy RJ (2003) Influenza virus induction of apoptotic and extrinsic mechanisms. *Int Rev Immunol* 22: 425–449.
- Chanturiya AN, Basanez G, Schubert U, Henklein P, Yewdell J W, et al. (2004) PB1-F2, an influenza A virus-encoded proapoptotic mitochondrial protein creates variably sized pores in planar lipid membranes. *J Virol* 78: 6304–6312.
- Bruns K, Studtucker N, Sharma A, Fossen T, Mitzner D, et al. (2007) Structural characterization and oligomerization of PB1-F2, a proapoptotic influenza A virus protein. *J Biol Chem* 282: 353–363.
- Chevalier C, Al Bazzal A, Vidic J, Fevier V, Bourdieu C, et al. (2010) PB1-F2 influenza A virus protein adopts a beta-sheet conformation and forms amyloid fibres in a membrane environment. *J Biol Chem* (in press).
- Henklein P, Bruns K, Nimitz M, Wray V, Tessmer U, et al. (2005) Influenza A virus protein PB1-F2: synthesis and characterization of the biologically active full length protein and related peptides. *J Peptide Sci* 11: 481–490.
- Killian JA, von Heijne G (2000) How proteins adapt to a membrane-water interface. *Trends Biochem Sci* 25: 429–434.
- Mitzner D, Dudek SE, Studtucker N, Anhlán D, Mazur I, et al. (2009) Phosphorylation of the influenza A virus PB1-F2 protein by PKC is required for effective virus propagation. *Cellular Microbiology* 1: 1502–1516.
- Hille B (2001) Ion channels of excitable membranes, Sinauer, Sunderland Massachusetts USA.
- Madan V, Castelló A, Carrasco L (2008) Viroporins from RNA viruses induce caspase-dependent apoptosis. *Cell Microbiol* 10: 437–451.
- Hessa T, White ST, van Heijne G (2005) Membrane insertion of a potassium-channel voltage sensor. *Science*. pp 307–1427.
- Herce HD, Garcia AE, Litt J, Kane RS, Martin P, et al. (2009) Arginine-rich peptides destabilize the plasma membrane, consistent with a pore formation translocation mechanism of cell penetrating peptides. *Biophys J* 97: 1917–1925.
- Binder H, Lindholm G (2003) Charge-dependent translocation of the Trojan peptide penetrating across lipid membranes. *Biophys J* 85: 982–995.
- Eisenberg M, Hall JE, Mead CA (1973) The nature of the voltage-dependent conductance induced by alamethicin in black lipid membranes. *J Membrane Biol* 14: 143–176.
- Fischer WB, Sansom MSP (2002) Viral ion channels: structure and function. *Biochem Biophys Acta* 152: 27–45.
- Gonzales ME, Carrasco L (2003) Viroporins. *FEBS Lett* 552: 28–34.
- Nieva JL, Agirre A, Nir S, Carrasco L (2003) Mechanisms of membrane permeabilization by picornavirus 2B viroporin. *FEBS Letters* 552: 68–73.
- Kovacs RJ, Nelson MT, Simmerman HK, Jones LR (1988) Phospholamban forms Ca<sup>2+</sup> selective channels in lipid bilayers. *J Biol Chem* 263: 18364–18368.
- Duclohier H, Wróblewski H (2001) Voltage-dependent pore formation and antimicrobial activity by alamethicin and analogues. *J Membrane Biol* 184: 1–12.
- Schrempf H, Schmidt O, Kummerlin R, Hinnah S, Muller D, et al. (1995) A prokaryotic potassium ion channel with two predicted transmembrane segments from *Streptomyces lividans*. *EMBO J* 14: 5170–5178.
- Montal M, Mueller P (1972) Formation of bimolecular membranes from lipid monolayers and a study of their electrical properties. *Proc Natl Acad Sci USA* 69: 3561–3566.
- Röder R, Brund K, Sharma A, Eissmann AA, Hahn F, et al. (2008) Synthesis of full length PB1-F2 influenza A virus proteins from 'spanish flu' and 'bird flu'. *J Peptide Science* 14: 954–962.
- Humphrey W, Dalke A, Schulten K (1996) VMD - Visual molecular dynamics. *J Molec Graphics* 14: 33–38.
- MacKerell AD, Jr., Bashford D, Bellott M, Dunbrack RL, Evansck JD, et al. (1998) All-atom empirical potential for molecular modelling and dynamics Studies of proteins. *J Phys Chem B* 102: 3586–3616.
- Schlenkerich M, Brickmann J, MacKerell AD, Jr., Karplus M (1996) An empirical potential energy function for phospholipids: criteria for parameter optimization and applications. In *Biological Membranes: A Molecular Perspective from Computation and Experiment* Merz. KM, Roux B, eds. Birkhäuser, Boston. pp 31–81.
- Jorgensen LW, Chandrasekhar J, Madura JD, Impey RW, Klein ML (1983) Comparison of simple potential functions for simulating liquid water. *J Chem Phys* 79: 926–935.
- Roux Lab Home Page (2006) Available: <http://thallium.bsd.uchicago.edu/RouxLab/>.
- Kale L, Skeel R, Bhandarkar M, Brunner R, Gursoy A, et al. (1999) NAMD2: greater scalability for parallel molecular dynamics. *J Comput Phys* 151: 283–312.
- Essmann U, Perera L, Berkowitz ML, Darden T, Lee H, et al. (1995) A smooth particle mesh Ewald method. *J Chem Phys* 103: 8577–8593.
- Tu K, Tobias DJ, Klein ML (1995) Constant pressure and temperature molecular dynamics simulation of a fully hydrated liquid crystal phase dipalmitoylphosphatidylcholine bilayer. *Biophys J* 69: 2558–2562.
- Feller SE, Zhang Y, Pastor RW, Brooks BR (1995) Constant pressure molecular dynamics simulation: the Langevin piston method. *J Chem Phys* 103: 4613–4621.
- Frishman D, Argos P (1995) Knowledge-based protein secondary structure assignment. *Proteins* 23: 566–579.